Equilibrium and Kinetic Studies of the Binding of Monoanionic and Dianionic Ligands to Bovine Serum Albumin

Kiyofumi MURAKAMI
Department of Chemistry, Faculty of Education, Yamaguchi University, Yoshida 1677-1, Yamaguchi 753
(Received March 15, 1993)

The binding of monoanionic azo dyes (4-(2-hydroxy-1-naphtylazo)benzenesulfonate (Orange II) and 6-hydroxy-5-phenylazo-2-naphthalenesulfonate (Ponceau 4G)) and dianionic one (6-hydroxy-5-(4-sulfophenylazo)-2-naphthalenesulfonate (Sunset Yellow FCF)) to bovine serum albumin (BSA) at pH=7.0 and 25 °C has been studied by equilibrium dialysis, spectrophotometry, and a temperature-jump method. The binding parameters for the monoanionic dyes were found to take quite similar values to each other. This shows that both of the dyes bind to BSA in essentially the same manner, irrespective of the difference in the position of the sulfonato group on the ligands. On the other hand, the data for the dianionic dye showed that the secondary sites, observed for the monoanionic dyes, almost completely disappeared, while the number and the binding constant for the primary sites were comparable. Kinetic data concerning the BSA–Sunset Yellow FCF system were found to be consistent with a scheme in which a bimolecular binding is followed by two isomerizations of the complex at the primary site. All of the equilibrium and rate constants for the scheme have been determined. A comparison of the results to those for other ligands has shown that the bimolecular association rate constant successively decreases with an increase in the number of anionic charges on the ligands. In the case of monoanionic dyes, however, the number of observed relaxations showed a tendency to increase with an increase in the number of bound dyes on the secondary sites. On the basis of these results, the detailed binding mechanism is discussed from the view point of the relation between the specificity of ligand-binding and the number of charges on the ligand.

Physicochemical studies concerning the relation between the ligand-binding mechanism of serum albumin and the structures of the protein and ligands are very important for understanding the inherent role of albumin molecules as the carrier and reservoir of many kinds of metals and organic molecules in blood.

From binding studies concerning many organic ligands, it has been learned that there are two kinds of binding modes: specific and nonspecific. The former means strong binding (the binding constant is typically in the range from 10^5 M^{-1} to 10^8 M^{-1} ($1\ M=1\ mol\,dm^{-3}$)) for a few distinct sites on albumin molecules, while the latter is relatively weak binding to many sites. Concerning specific binding, the binding regions and locations of binding sites on albumin molecules have recently been explored.[1—4] On the basis of these results and a three-dimensional model of the domain structure of albumin,[5] the detailed nature of the specific binding sites has been examined.[6] These results have also been confirmed by a quite recent crystallographic study of the three-dimensional structure of human serum albumin (HSA).[7] Furthermore, kinetic studies have also revealed the detailed mechanism through a clarification of the binding scheme.[8—20] However, the structural requisites for the specific or nonspecific binding have not been fully clarified.

Monoanionic azo dyes such as sodium 4′-dimethylaminoazobenzene-4-sulfonate (Methyl Orange)[21,22] and sodium 4-(4-hydroxy-1-naphthylazo)-benzenesulfonate (Orange I)[23] are known to bind to bovine serum albumin (BSA) in a typically nonspecific manner. On the other hand, trianionic and tetranionic azo dyes show a fairly specific binding,[20] in which the binding constant for the primary site progressively increases with an increase in the number and density of anionic charges on the ligand. These results seem to suggest that the number of anionic charges on ligands play an important role concerning the binding specificity.

The present paper describes the equilibrium and kinetic properties of the binding of monoanionic and dianionic azo dyes (which have the same back born structure) to BSA, and shows the relation between the ligand-binding specificity of BSA and the number of anionic charges on the ligand.

Experimental

Materials. Bovine serum albumin (Fatty acid free <0.02%) was purchased from Armour, and was used without further purification. The molar concentration of BSA solutions was determined from the absorbance at 280 nm ($E^{1\%}_{1cm}=6.6$[24]), assuming a molecular weight of 67 kDa ($1\ Da\approx 1.66054\times10^{-27}$ kg). Sodium 4-(2-hydroxy-1-naphtylazo)benzenesulfonate (Orange II) was purchased from Wako Pure Chemical industries, and sodium 6-hydroxy-5-phenylazo-2-naphthalenesulfonate (Ponceau 4G) and disodium 6-hydroxy-5-(4-sulfophenylazo)-2-naphthalenesulfonate (Sunset Yellow FCF) were obtained from Tokyo Chemical Industry Co., Ltd. These were purified by three-times recrystallizations from each of an aqueous sodium acetate solution and an aqueous ethanol solution, and dried at 115 °C in a vacuum for 20 h. Figure 1 illustrates the chemical structures of these dyes. From a series of spectrophotometric titrations, the pK_a values of the hydroxyl group of these dyes were found to be larger than 10; no spectral change was observed over the pH range from 3 to 9. From the concentration dependence of the absorption spectrum at pH=7.0, the molar extinction coefficients of these dyes at infinite dilution were determined to

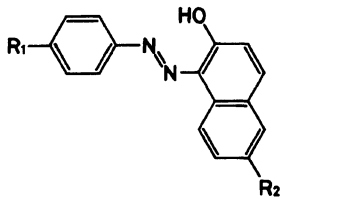

Dye	R_1	R_2
Orange II	SO_3Na	H
Ponceau 4G	H	SO_3Na
Sunset Yellow FCF	SO_3Na	SO_3Na

Fig. 1. Chemical structure of dyes.

be $\varepsilon_{484}=2.37\times10^4$ $M^{-1}cm^{-1}$ (Orange II), $\varepsilon_{480}=2.07\times10^4$ $M^{-1}cm^{-1}$ (Ponceau 4G), and $\varepsilon_{480}=2.39\times10^4$ $M^{-1}cm^{-1}$ (Sunset Yellow FCF). All of the other chemicals used were reagent-grade. All of the sample solutions were prepared in a 0.1 M Na_2HPO_4–NaH_2PO_4 buffer of pH=7.00±0.02.

Methods. The extent of binding was determined by the use of an equilibrium dialysis technique. The details concerning the technique have been reported elsewhere.[20] Spectrophotometric measurements were carried out with Shimadzu UV-200S and UV-100 spectrophotometers. Temperature-jump measurements were performed with a Unisoku TF-102 fluorescence temperature-jump spectrophotometer. The data were obtained at a temperature rise of 5 °C. The details concerning the apparatus can be found elsewhere.[25] All of the experiments were performed at 25±0.2°C. The calculations were accomplished with an Acos-850 computer system (NEC Corporation).

Results and Discussion

Binding Parameters. Figure 2 illustrates Scatchard plots[26] of the binding of Orange II, Ponceau 4G, and Sunset Yellow FCF to BSA at pH=7.0 and 25 °C. These curved plots show that BSA has at least two classes of binding sites for each ligand. Assuming that all of the binding sites are independent of each other, the number of moles of the ligand bound per molecule of the protein ($\bar{\nu}$) can be expressed by[27]

$$\bar{\nu}=\frac{n_1K_1^*L}{1+K_1^*L}+\frac{n_2K_2^*L}{1+K_2^*L}, \quad (1)$$

where n, K^*, and L are the number of binding sites, the binding constant and the free ligand concentration, respectively; subscripts 1 and 2 refer, respectively, to the primary and secondary binding sites. The data were fitted to Eq. 1 by a nonlinear regression analysis.[28] The values of the determined binding parameters are listed in Table 1.

From Table 1, we can see the following points. The values of the binding parameters for the monoanionic dyes (Orange II and Ponceau 4G) are quite similar to each other; that is, the binding parameters does not depend on whether the sulfonato group is located at the benzene ring or at the naphtalene ring. However, for Sunset Yellow FCF, which has two sulfonato groups at

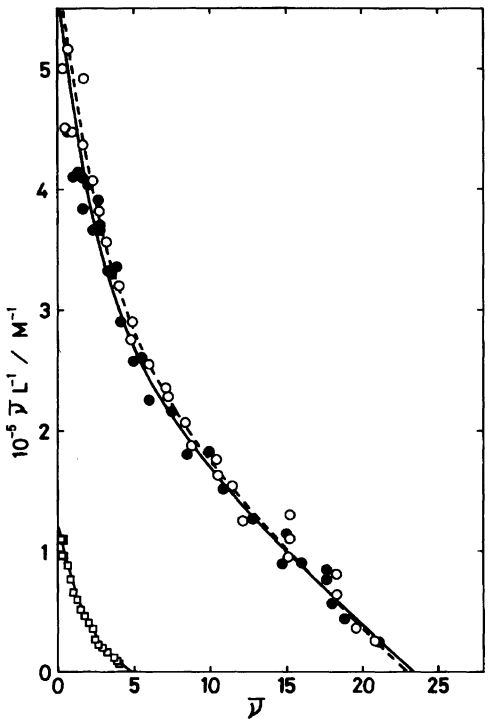

Fig. 2. Scatchard plots of the interaction between BSA and Orange II (○), Ponceau 4G (●), and Sunset Yellow FCF (□) at 25 °C and pH=7.0. The data were obtained for a BSA concentration of 5×10^{-5} M. The solid lines represent the theoretical curves calculated from the values of the binding parameters listed in Table 1.

Table 1. Binding Parameters

Dye	n_1	$10^{-5}K_1^*$ / M^{-1}	n_2	$10^{-4}K_2^*$ / M^{-1}
Orange II	2.01	1.80	20.8	1.13
Ponceau 4G	1.98	1.73	21.4	1.06
Sunset Yellow FCF	1.6	0.62	3.2	0.60

The accuracy of the parameters for Orange II and Ponceau 4G was estimated to be between ±3%, and that for Sunset Yellow FCF was between ±25%.

the both positions, the number of secondary sites is extremely reduced compared to that of monoanionic dyes (from 21 to 3), while the parameters for the primary sites are comparable to those of monoanionic ligands.

Binding Modes. As was noted in the introduction, two kinds of binding mode (specific and non-specific bindings) are known for the binding of organic ligands to albumin. If strong binding to one or a few sites is predominant in the overall binding of a ligand, the binding is called specific. On the contrary, the case in which there exists equivalent many relatively weak binding sites is typically nonspecific. Both of the modes can be available for a ligand, though their relative weight is dependent on the ligand structure.

For specific binding, Brown and Shockley[6] have vi-

sualized the possible structure of the binding sites; this involves "mouths" of a double funnel-shaped domain, which contain a cluster of basic residues, and is further able to offer a hydrophobic environment in their interior. This structural feature has been ascertained from the crystallographic study of HSA,[7] in which two principal ligand-binding regions are shown to be located in subdomains IIA and IIIA. These mouths may provide two primary sites for the present ligands.

However, the nonspecific binding sites observed for Orange II and Ponceau 4G in the present study as the secondary sites, and for Methyl Orange[21,22] and Orange I[23] could not be fully interpreted in terms of the existence of such "mouths", since the number of such mouths per one protein molecule is inferred as being at most 6.[5,6] Other possible sites must therefore be proposed. The common structural aspect of these dyes is that they have one negatively charged sulfonato group and a relatively large hydrophobic part. Both of these seem to contribute to the stabilization of the complex at the nonspecific binding sites through an electrostatic interaction between the sulfonato group and a positive charge on basic residues, and through a hydrophobic interaction between the hydrophobic parts of the ligand and the protein. This is because the values of the binding constant (on the order of 1×10^4 M^{-1}) is, for the reason given in the next paragraph, too large to ascribe them solely to an electrostatic interaction.

The value of the association constant due to the electrostatic interaction between the sulfonato group of the ligands and the cationic group of the basic residues, such as lysine and arginine etc., can be estimated by the theory of ion association[29] as being

$$K = \left(8\pi Na^3/1000\right)\sum_{n=1}^{\infty} b^{2n+2} \Big/ \left[(2n+2)!(2n-1)\right], \quad (2)$$

where a, b, and N are the closest distance of approach of the ions, Bjerrum's parameter and Avogadro's number, respectively. Assuming that a=4 Å and ε=78.3, i.e., the cationic groups of the basic residues would be exposed to the solvent, the value of K becomes 0.44 M^{-1} from Eq. 2. Even if the value of local dielectric constant is reduced to 20, the value of K is at most on the order of 100 M^{-1}. In practice, similar values are reported for the binding of Cl^{-1}, I^-, and SCN^- to BSA,[30] in which the electrostatic interaction must play a central role.

It is therefore reasonable to assume that the nonspecific binding sites comprise one positively charged residue, at least, and a hydrophobic crevice or a patch located in the vicinity of the residue. This model is also capable interpreting the fact that the nonspecific binding sites almost perfectly disappear for Sunset Yellow FCF, which has two sulfonato groups at the benzene and naphtalene rings, by supposing that the second sulfonato group prohibits an approach of the hydrophobic part of the ligand to the hydrophobic crevice or the patch. If the detailed surface structure of albumin molecules becomes known from crystallographic data,[7] possible locations and the nature of the nonspecific binding sites will become more clear.

Kinetics of BSA–Sunset Yellow FCF System. Three distinct relaxations have been observed for the BSA–Sunset Yellow FCF system (Fig. 3). The wave lengths for the kinetic measurements were selected so as to give a good signal-to-noise ratio. As can be seen from the results of an equilibrium dialysis (Table 1), the magnitude of the binding ability of the primary sites (n_1K_1*) is about five-times as large as that of the secondary sites (n_2K_2*). It is therefore reasonable to assume that the observed relaxations are due to the primary sites. Figure 4 shows the dependence of the reciprocal relaxation times on the sum of the equilibrium concentrations of free primary sites and a free ligand ($P+L$), which was calculated using the values of the binding parameters. We can see from this figure that τ_1^{-1} increases linearly with ($P+L$) (Fig. 4(A)), and that τ_2^{-1} and τ_3^{-1} increase with ($P+L$) and reach plateau values at high values of ($P+L$) (Fig. 4(B) and 4(C)). This behavior of the relaxation times suggests a scheme in which a bimolecular binding between free primary sites and free ligand is followed by two isomerizations of the complex, as the simplest one:

$$\mathrm{P+L} \underset{k_{-1}}{\overset{K_1\ (k_1)}{\rightleftharpoons}} \mathrm{C_1} \underset{k_{-2}}{\overset{K_2\ (k_2)}{\rightleftharpoons}} \mathrm{C_2} \underset{k_{-3}}{\overset{K_3\ (k_3)}{\rightleftharpoons}} \mathrm{C_3}\ . \quad (3)$$

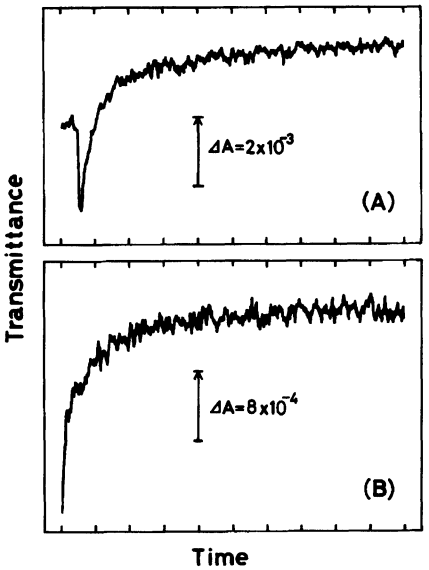

Fig. 3. Typical temperature-jump relaxation curves observed for the BSA–Sunset Yellow FCF system at 25 °C and pH=7.0, $L_0=2\times10^{-5}$ M, and $P_0/L_0=1$. The wavelength and horizontal scale are (A) λ=480 nm, 1 ms per division, (B) λ=480 nm, 25 ms per division. The arrow designated for each curve shows the direction and magnitude of the positive absorbance change.

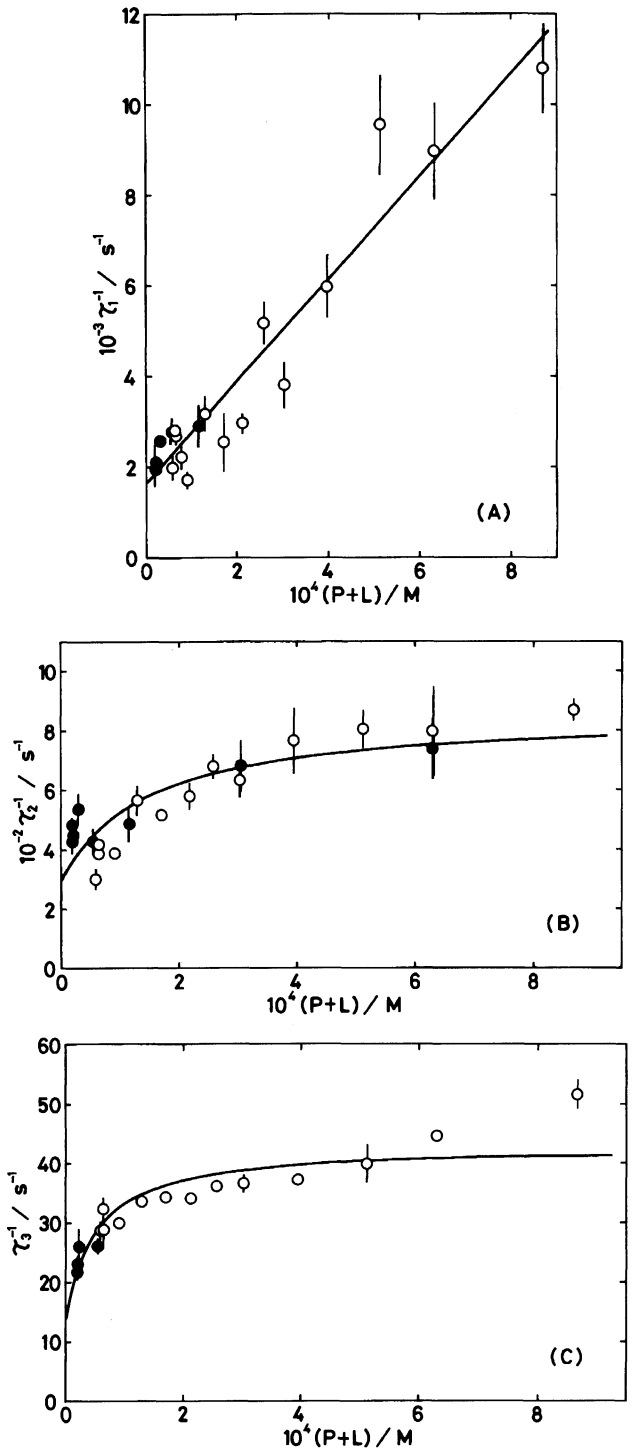

Fig. 4. Plots of τ_1^{-1} (A), τ_2^{-1} (B), and τ_3^{-1} (C) vs. the sum of the equilibrium concentrations of free primary sites and free ligands for the BSA–Sunset Yellow FCF system. The open circles show the data collected for the L_0 values from 5×10^{-6} M to 1×10^{-3} M at $P_0=5\times10^{-5}$ M, and closed ones show the data for P_0 values from 2×10^{-6} M to 4×10^{-4} M at $L_0=2\times10^{-5}$ M. The solid lines represent the theoretical curves (Eqs. 4, 5, and 6) calculated from the values of the equilibrium and rate constants listed in Table 2 (see text).

This scheme predicts the reciprocal relaxation times for each of the three steps as[31]

$$\tau_1^{-1} = k_1(P+L) + k_{-1}, \tag{4}$$

$$\tau_2^{-1} = k_2\frac{K_1(P+L)}{1+K_1(P+L)} + k_{-2} \tag{5}$$

and

$$\tau_3^{-1} = k_3\frac{K_1K_2(P+L)}{1+K_1(1+K_2)(P+L)} + k_{-3}. \tag{6}$$

On the basis of these equations, the data were analyzed by the following procedure. At first, the data of τ_1^{-1} in Fig. 4(A) were fitted to Eq. 4 by a linear least-squares analysis to obtain k_1 and k_{-1}. The value of the equilibrium constant of the first step was then determined from $K_1=k_1/k_{-1}$. Using this value of K_1, the value of the factor $K_1(P+L)/\{1+K_1(P+L)\}$ in Eq. 5 was calculated for each data point in Fig. 4(B); subsequently, k_2 and k_{-2} were determined by fitting the data to Eq. 5 by the least-squares analysis. The value of K_2 was also determined from $K_2=k_2/k_{-2}$. Using the thus-determined values of K_1 and K_2, the value of the factor $K_1K_2(P+L)/\{1+K_1(1+K_2)(P+L)\}$ in Eq. 6 was then determined for each point in Fig. 4(C); finally, the values of k_3, k_{-3} and $K_3(=k_3/k_{-3})$ were determined by the same method. The results are summarized in Table 2, and the theoretical curves for the reciprocal relaxation times calculated using these values are illustrated in Fig. 4 as the solid curves. Using the kinetically determined values of the equilibrium constants for the steps in Eq. 3, the value of the over-all association constant can be estimated as

$$K\ (\text{over all}) = K_1 + K_1K_2 + K_1K_2K_3 = 7.7\times10^4\ \text{M}^{-1}. \tag{7}$$

Considering the accuracy estimated for the equilibrium and kinetic parameters, this value is regarded as being in agreement with the value of the binding constant for the primary sites in Table 1. This agreement shows a self-consistency of the present analysis, and confirms the validity of the proposed scheme.

Table 3 shows the now-available data for the bimolecular association rate constants of albumin-ligand systems, which were obtained through an observation of the process as the distinct one and for ligands having similar structures to the present ligands. It can

Table 2. Kinetic Parameters for the Binding of Sunset Yellow FCF to the Primary Site on BSA

K_1	k_1	k_{-1}	K_2	k_2	k_{-2}	K_3	k_3	k_{-3}
M^{-1}	$M^{-1}s^{-1}$	s^{-1}		s^{-1}	s^{-1}		s^{-1}	s^{-1}
7.6×10^3	1.3×10^7	1.7×10^3	2.0	580	300	3.7	47	13

The accuracy of the parameters was estimated to be between ±19%.

Table 3. Association Rate Constants for BSA–Ligand Systems

Ligand	Number of anionic charges on ligand	Association rate constant $M^{-1}s^{-1}$	Reference
ANS	1	$2—5\times10^8$	(32)
Orange I	1	2.4×10^8	(23)
Sunset yellow FCF	2	1.3×10^7	This work
Ponceau 4R	3	3.5×10^6	(20)

be seen that the rate constants for the monoanionic ligands take similar values to each other. As discussed by Regenfuss and Clegg,[32] these values are about one-tenth of that expected for a spherically symmetric diffusion-controlled association ($k=6\times10^9$ $M^{-1}s^{-1}$). They have reasonably ascribed this to the small reactive area of one site on the protein surface. However, this could not solely interpret the other fact (which can also be deduced from Table 3) that the association rate constant progressively decreases with an increase in the number of anionic charges on the ligand. This fact suggests that some restricted orientation of the ligand is required for the approach of multicharged ligands to the sites. In this context, the result of the previously cited crystallographic study is noticeable, that the entrance of the two possible primary sites contains three or four cationic residues.[7] The electrostatic potential due to these cationic residues would be one of the determining factors for the orientation state.

Comparing the values of the kinetic parameters for the second and third steps with those of the trianionic and tetranionic ligands,[20] we can see that the intramolecular reactions of the complex are quite similar to those of the BSA–Amaranth system, except that the value of the backward rate constant of the second step of the BSA–Sunset Yellow FCF system is about three-times larger than that of the BSA–Amaranth system. This shows that in spite of the differences in the number and position of anionic charges on the ligands and in the backbone structure, both of the BSA–dye complexes are formed by the same mechanism.

Kinetics of BSA–Orange II, BSA–Ponceau 4G Systems. Figures 5 and 6 show plots of the reciprocal relaxation times vs. $\bar{\nu}$, determined for BSA–Orange II and BSA–Ponceau 4G systems. In the case of the BSA–Orange II system, one relaxation (τ_2), observed at $\bar{\nu}<0.5$, splits into two (τ_{21}, τ_{22}) in the region of $0.5<\bar{\nu}<4$, and again becomes one at $4<\bar{\nu}$. Another fast relaxation (τ_1) becomes observable at $1<\bar{\nu}$. In the case of the BSA–Ponceau 4G system, on the other hand, two relaxations (τ_1, τ_2) were observed at $\bar{\nu}<1$. The fast one (τ_1) of these splits into two (τ_{11}, τ_{12}) in the region $1<\bar{\nu}<4$; one of these (τ_{11}) splits further into two (τ_{111}, τ_{112}) at $4<\bar{\nu}$. Another slow relaxation (τ_3) becomes observable at $\bar{\nu}=16$. By comparing the values of τ^{-1}'s between these systems, it may be concluded that the τ_2's at $\bar{\nu}<1$ for both systems originate from the same mode of isomerization. It also seems likely that τ_1 of

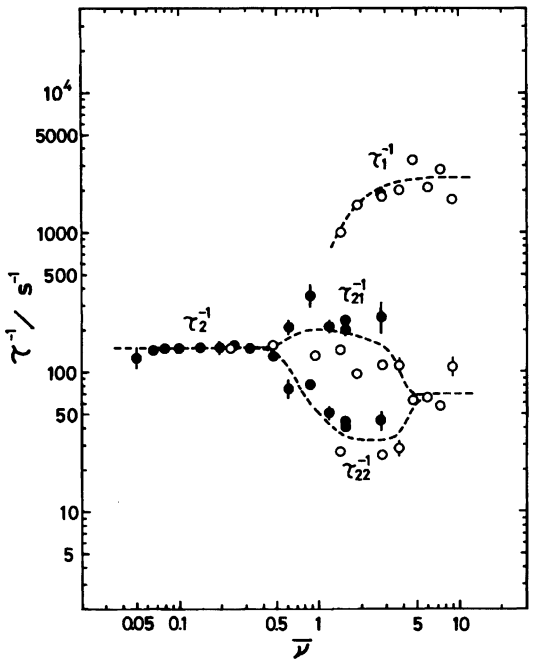

Fig. 5. Plot of reciprocal relaxation times vs. $\bar{\nu}$ for the BSA–Orange II system. The open circles show the data collected for the L_0 values from 5×10^{-6} M to 1×10^{-3} M at $P_0=5\times10^{-5}$ M, and closed ones show the data for P_0 values from 2×10^{-6} M to 4×10^{-4} M at $L_0=2\times10^{-5}$ M.

the BSA–Orange II system and τ_{11} of the BSA–Ponceau 4G system have the same origin. By carrying out calculations using the binding parameters (Table 1), it was found that for both systems and for all of the reactant concentrations the amounts of bound ligands on the primary sites and on the secondary sites are either comparable to each other, or the latter is larger than the former. We therefore could not attribute the observed relaxations solely to one of the two classes of binding sites. Taking account of the relatively small number of primary sites ($n_1=2$), it is reasonable, however, to conclude that the splittings of the relaxations and the appearance of the new relaxation observed at higher $\bar{\nu}$ values are due to binding to the secondary sites. Therefore, the full binding scheme for these systems must be expressed by a combination of many bimolecular bindings to the primary and secondary sites and several isomerizations of the complexes. Although further details concerning the mechanism could not be clarified from only the present data, it is notable that these kinetic

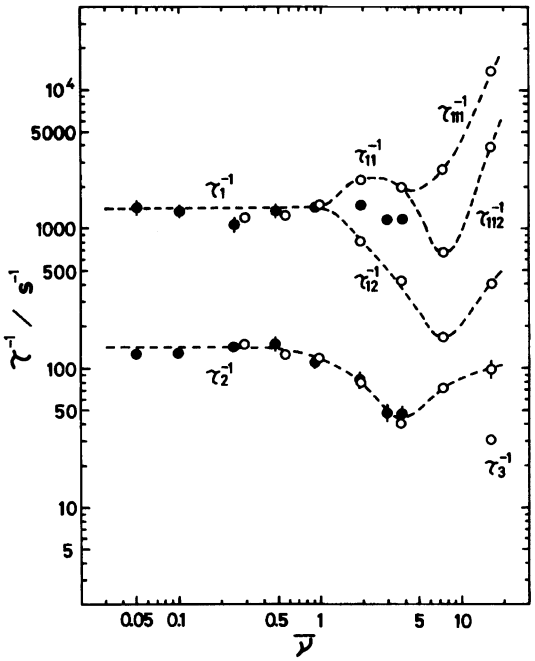

Fig. 6. Plot of reciprocal relaxation times vs. $\bar{\nu}$ for the BSA–Ponceau 4G system. The open circles show the data collected for the L_0 values from 5×10^{-6} M to 1×10^{-3} M at $P_0=5\times10^{-5}$ M, and closed ones show the data for P_0 values from 2×10^{-6} M to 4×10^{-4} M at $L_0=2\times10^{-5}$ M.

properties are very similar to those for the BSA–Orange I system, which is the typical nonspecific binding case.[23]

In summary, it was found that as the number of anionic charges on the ligands increases, the ligand-binding specificity of BSA tends to change from a nonspecific nature to a specific nature, and that the binding scheme also changes from a scheme having a complex nature to simple sequential binding at the primary sites.

References

1) Kragh-Hansen, *Pharmacol. Rev.*, **33**, 17 (1981).
2) Kragh-Hansen, *Dan. Med. Bull.*, **37**, 57 (1990).
3) K. J. Fehske, *Biochem. Pharmacol.*, **30**, 687 (1981).
4) T. Peters, Jr., *Adv. Protein Chem.*, **37**, 161 (1985).
5) J. R. Brown, "Albumin Structure, Function, and Uses," ed by V. M. Rosenoer, M. Oratz, and M. A. Rothschild, Pergamon Press, New York (1977), p. 27.
6) J. R. Brown and P. Shockley, "Lipid–Protein Interaction," ed by P. C. Jost and O. H. Griffith, John Wiley & Sons, New York (1982), Vol. 1, p. 25.
7) X. M. He and D. C. Carter, *Nature*, **358**, 209 (1992).
8) A. Froese, A. H. Sheon, and M. Eigen, *Can. J. Chem.*, **40**, 1786 (1962).
9) R. F. Chen, *Arch. Biochem. Biophys.*, **160**, 106 (1974).
10) T. Faerch and J. Jacobsen, *Arch. Biochem. Biophys.*, **184**, 282 (1977).
11) R. G. Reed, *J. Biol. Chem.*, **252**, 7483 (1977).
12) R. D. Gray and S. D. Stroupe, *J. Biol. Chem.*, **253**, 4370 (1978).
13) W. Scheider, *Proc. Natl. Acad. Sci. U.S.A.*, **76**, 2283 (1979).
14) W. Scheider, *J. Phys. Chem.*, **84**, 925 (1980).
15) N. Reitbrock and A. Labmann, *Naunyn-Schmiedeberg's Arch. Pharmacol.*, **313**, 269 (1980).
16) P. A. Adams and M. C. Berman, *Biochem. J.*, **191**, 95 (1980).
17) K. Murakami, T. Sano, and T. Yasunaga, *Bull. Chem. Soc. Jpn.*, **54**, 862 (1981).
18) K. Murakami, T. Sano, S. Tuchie, and T. Yasunaga, *Biophys. Chem.*, **21**, 127 (1985).
19) K. Murakami, Y. Kubota, Y. Fujisaki, and T. Sano, *Bull. Chem. Soc. Jpn.*, **59**, 3399 (1986).
20) K. Murakami, *Biophys. Chem.*, **41**, 253 (1991).
21) I. M. Klotz, F. M. Walker, and R. B. Pivan, *J. Am. Chem. Soc.*, **68**, 1486 (1946).
22) K. Shikama, *J. Biochem.* (*Tokyo*), **64**, 55 (1968).
23) K. Murakami, *Bull. Chem. Soc. Jpn.*, **61**, 1323 (1988).
24) E. J. Cohn, W. L. Huges, Jr., and J. H. Weare, *J. Am. Chem. Soc.*, **69**, 1753 (1947).
25) K. Murakami, K. Mizuguchi, Y. Kubota, and Y. Fujisaki, *Bull. Chem. Soc. Jpn.*, **59**, 3393 (1986).
26) G. Scatchard, *Ann. N. Y. Acad. Sci.*, **51**, 660 (1949).
27) J. Steinhardt and J. A. Reynolds, "Multiple Equilibria in Proteins," Academic Press, New York (1969), p. 15.
28) T. Nagasawa and Y. Oyanagi, "Recent Developments in Statistical Inference and Data Analysis," ed by K. Matsusita, North Holland, New York (1980), p. 221.
29) H. Yokoyama and H. Yamatera, *Bull. Chem. Soc. Jpn.*, **48**, 1770 (1975).
30) J. Steinhardt and J. A. Reynolds, "Multiple Equilibria in Proteins," Academic Press, New York (1969), p. 316.
31) C. F. Bernasconi, "Relaxation Kinetics," Academic Press, New York (1976), p. 43.
32) P. Regenfuss and R. M. Clegg, *Biophys. Chem.*, **26**, 83 (1987).